Ultrasound in Med. & Biol., Vol. 39, No. 1, pp. 172–180, 2013

0301-5629/$ - see front matter

http://dx.doi.org/10.1016/j.ultrasmedbio.2012.08.016

● *Original Contribution*

AN ANIMAL MODEL ALLOWING CONTROLLED RECEPTOR EXPRESSION FOR MOLECULAR ULTRASOUND IMAGING

Reshu Saini,* Anna G. Sorace,* Jason M. Warram,† Marshall J. Mahoney,* Kurt R. Zinn,†‡§ and Kenneth Hoyt*†‡§

*Department of Biomedical Engineering; †Department of Radiology; ‡Department of Electrical and Computer Engineering; and §Comprehensive Cancer Center, University of Alabama at Birmingham, Birmingham, AL, USA

(*Received* 8 *December* 2011; *revised* 3 *August* 2012; *in final form* 21 *August* 2012)

Abstract—Reported in this study is an animal model system for evaluating targeted ultrasound (US) contrast agents binding using adenoviral (Ad) vectors to modulate cellular receptor expression. An Ad vector encoding an extracellular hemagglutinin (HA) epitope tag and a green fluorescent protein (GFP) reporter was used to regulate receptor expression. A low and high receptor density (in breast cancer tumor bearing mice) was achieved by varying the Ad dose with a low plaque forming unit (PFU) on day 1 and high PFU on day 2 of experimentation. Targeted US contrast agents, or microbubbles (MB), were created by conjugating either biotinylated anti-HA or IgG isotype control antibodies to the MB surface with biotin-streptavidin linkage. Targeted and control MBs were administered on both days of experimentation and contrast-enhanced US (CEUS) was performed on each mouse using MB flash destruction technique. Signal intensities from MBs retained within tumor vasculature were analyzed through a custom Matlab program. Results showed intratumoral enhancement attributable to targeted MB accumulation was significantly increased from the low Ad vector dosing and the high Ad vector dosing ($p = 0.001$). Control MBs showed no significant differences between day 1 and day 2 imaging ($p = 0.96$). Additionally, targeted MBs showed a 10.5-fold increase in intratumoral image intensity on day 1 and an 18.8-fold increase in image intensity on day 2 compared with their control MB counterparts. (E-mail: hoyt@uab.edu) © **2013 Published by Elsevier Inc. on behalf of World Federation for Ultrasound in Medicine & Biology.**

Key Words: **Adenoviral vectors, Modulated receptors, Contrast-enhanced ultrasound imaging, Microbubbles.**

INTRODUCTION

Molecular imaging is now a heralded approach for visualizing cellular level processes within the body. Magnetic resonance (MR), positron emission tomography (PET), single positron emission computed tomography (SPECT) and ultrasound (US) have emerged as the leading modalities in this field. With the help of contrast agents, molecular ultrasound imaging allows for a noninvasive examination of pathologies (Pysz et al. 2010a, 2011). Increased knowledge on the effects and processes of various diseases facilitates new detection, monitoring and therapeutic techniques.

Ultrasound has become a promising molecular imaging modality because of real-time capabilities and nonionizing radiation exposure. Being relatively inexpensive and widely available positions US as an attractive alternative to other imaging systems. With the introduction of microbubble (MB) contrast agents, the sensitivity and specificity of US for detecting pathologies has greatly improved over the last decade (Pysz et al. 2011). Composed of a stable lipid or protein outer shell and a low diffusivity gaseous core, MBs provide an acoustic impedance mismatch compared with the surrounding blood, thus, enhancing US backscatter signals (Leighton 1997). Targeting MBs to specific endothelial markers that are expressed in certain pathologic states has shown improved contrast enhancement *via* local accumulation (Klibanov 2005). Targeted MBs have been applied to different fields including inflammation (Bachmann et al. 2006; Ferrante et al. 2009; Kaufmann et al. 2009), tumor angiogenesis (Willmann et al. 2010; Warram et al. 2011, 2012; Knowles et al. 2012) and intravascular thrombi (Schumann et al. 2002; Wang et al. 2006; Kaufmann 2009).

Expanding the range of receptor density levels within a particular cell line could permit more detailed

Address correspondence to: Kenneth Hoyt, Ph.D., M.B.A., Department of Radiology, University of Alabama at Birmingham, G082 Volker Hall, 1670 University Boulevard, Birmingham, AL 35294, USA. E-mail: hoyt@uab.edu

targeted MB studies of binding dynamics. Therefore, molecular US imaging studies could benefit from reproducible control of cell surface target protein density. An adenovirus (Ad) vector has been developed where the expression level of an extracellular hemagglutinin (HA) epitope tag and green fluorescent protein (GFP) optical imaging reporter are dependent on infectious Ad dose level (viral plaque forming units or PFU) (Zinn et al. 2002). A previous study by our group assessed the feasibility of using this Ad-HA-GFP vector for selectively changing receptor levels targeted using antibody-labeled MBs (Saini et al. 2011). Importantly, anti-HA antibody-labeled MB binding was shown to be linearly proportional to target HA expression in this model system. In the present study, the same Ad vector infectivity techniques were used to explore molecular US imaging of targeted MBs in an animal model system.

METHODS AND MATERIALS

Cell culture

2LMP (MDA-MB-231 lung metastatic pooled) breast cancer cells were grown in Dulbecco's modified Eagles medium without phenol red (Mediatech, Inc., Manassas, VA, USA) with 10% FBS (HyClone, Loga, UT, USA) and 1% L-Glutamine. At 80%–90% confluency, cells were trypsinized and counted with a hemocytometer for *in vivo* assays. Cell viability was also determined using trypan dye exclusion. All cells were cultured in 37°C with 5% CO_2.

Animal preparation

All animal protocols were approved by Institutional Animal Care and Use Committee (IACUC) at the University of Alabama at Birmingham. Female nude athymic mice ($N = 18$) were obtained from Frederick Cancer Research (Hartford, CT, USA). 2MLP breast cancer cells (2×10^6) in a 0.2 mL solution of phosphate buffered saline (PBS) were implanted subcutaneously in the right flank of each mouse. Four weeks post-implantation each animal was injected intratumorally with 0.1 mL of an Ad-HA-GFP vector at a relatively low concentration of 1×10^6 PFU/tumor to induce intratrumoral HA expression unless otherwise noted. For completeness, Figure 1a illustrates HA surface expression following cell infection using the Ad vector. The Ad vector was injected in 10 different sites within the tumor approximately 0.01 mL per site to maximize probability of delivering a homogenous dose. This day 0 injection was considered a low dose PFU. Our group has shown previously that tumors injected with the Ad-HA-GFP vector can be visualized within 24 h by gamma camera imaging and that maximum expression was localized to the tumor (Rogers et al. 2003). Molecular imaging was performed 24 h after Ad dosing (low Ad dose, day 1). After imaging, animals were re-injected with an increased virus concentration of 1×10^9 PFU/tumor using the same technique as discussed above (high Ad dose, day 2). Again, molecular imaging was repeated 24 h after Ad dosing.

Targeted contrast agent preparation

Contrast agents were prepared as previously reported (Saini et al. 2011). Briefly, targeted MBs were made by conjugating biotinylated antibodies onto a streptavidin coated MB (Targetsar-SA, Targeson, San Diego, CA, USA). Monoclonal biotinylated anti-HA (Sigma Aldrich, St. Louis, MO, USA) or IgG isotype control (Southern Biotech, Birmingham, AL, USA) antibodies (100 μg) were incubated with the streptavidin-coated MB for 20 min followed by a centrifugal washing at $\times$400 for 4 min. Final solutions of each MB group were diluted with PBS to a total volume of 1.0 mL and the final concentration was characterized using a hemacytometer and reported as MBs per mL. MB size was reported to be 2.51 ± 0.03 μm according to the manufacturer. Figure 1b illustrates the concept of HA-targeted MB flow within a blood vessel following Ad-HA-GFP vector infection, where these MBs exhibit specific binding to the induced receptors.

Ultrasound imaging

Molecular US imaging of tumor-bearing animals ($N = 6$) was performed after infection (both low and high Ad dosing) in a water bath maintained at 37°C. All animals were maintained under isoflurane anesthesia during entirety of the imaging. Pulse inversion harmonic imaging of targeted MBs was performed using a SONIX RP US system (Ultrasonix Medical Corp, Richmond, BC) equipped with a L12-4 linear array transducer at a mechanical index (MI) of 0.1. Transmit and receive frequency were set to 5 MHz and 10 MHz, respectively, and the dynamic range setting was fixed to 70 dB. The largest transverse cross-sectional area was identified for animal tumor prior to US imaging along that plane. The acoustic focus was set proximal to the tumor while US system parameters were fixed for all imaging sessions. On day 1, all mice were administered control MBs *via* a tail vein bolus injection of 0.05 mL MB solution (1.0×10^7 MB/mouse) and 0.05 mL saline (total dose of 0.1 mL). Following agent injection, a 2-min delay period allowed systemic MB circulation and an opportunity for binding to tumor vascularity (Warram et al. 2011; Knowles et al. 2012). Subsequently, US image sequences were acquired for 10 s and then a MB destruction "flash" sequence ($N = 10$ frames) was administered with an MI of 1.2 to destroy both circulating and attached MBs in the imaging plane. US images were then collected for another 20 s to capture tumor reperfusion of the MB

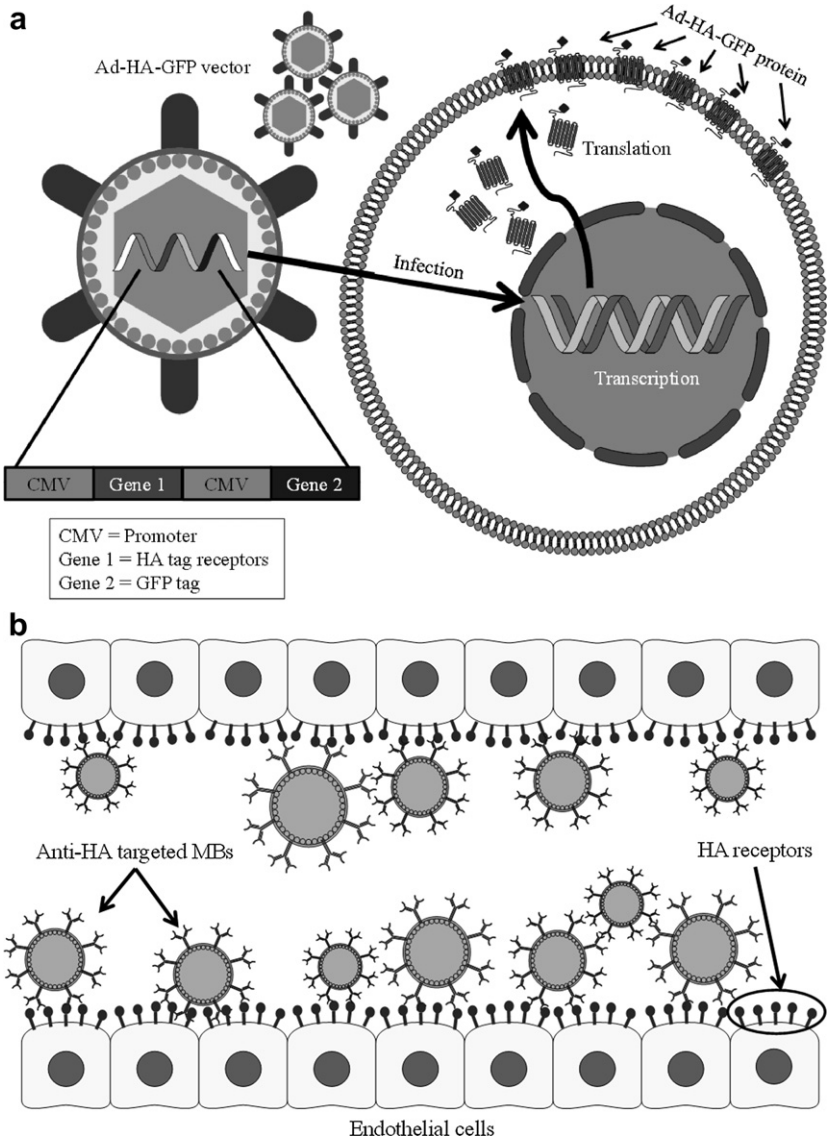

Fig. 1. (a) Basic schematic of the adenoviral (Ad) infection and translation of viral genome to produce Ad-HA-GFP proteins and (b) Depiction of HA targeted microbubbles (MBs) attaching to the Ad vector-induced HA receptors while flowing through the tumor vasculature. Ad-HA-GFP = adenoviral-hemagglutinin-green fluorescent protein.

contrast agents. Following a 1 h period for control MB clearance, targeted MBs were administered (1.0×10^7 MB/mouse in a 0.1 mL dosing) to the same animal population and molecular US imaging was repeated as described above. Day 2 imaging, after high Ad-HA-GFP vector dosing, was performed in all animals again using the same imaging protocol. All image data was saved as pre-scan converted images for offline processing.

Data analysis

Custom programs were developed using the Matlab software package (Mathworks Inc., Natick, MA, USA) for processing US image data. After user placement of a circular region-of-interest (ROI) with varying diameter to encompass the tumor, pixel intensities from pre-flash frames were digitally subtracted from the post-flash frames. The mean video intensity difference (arbitrary units) was calculated to determine the bound MB quantity. An illustration detailing quantification of MB binding to target receptors is presented in Figure 2.

Receptor characterization and immunohistology

All animals were humanely euthanized and tumors surgically excised for further analysis. For animals not subjected to the molecular US imaging study, fluorescence imaging of the GFP reporter signal (IVIS Imaging System 200 Series, Caliper Life Sciences, Hopkinton, MA, USA) on excised tumor samples was performed

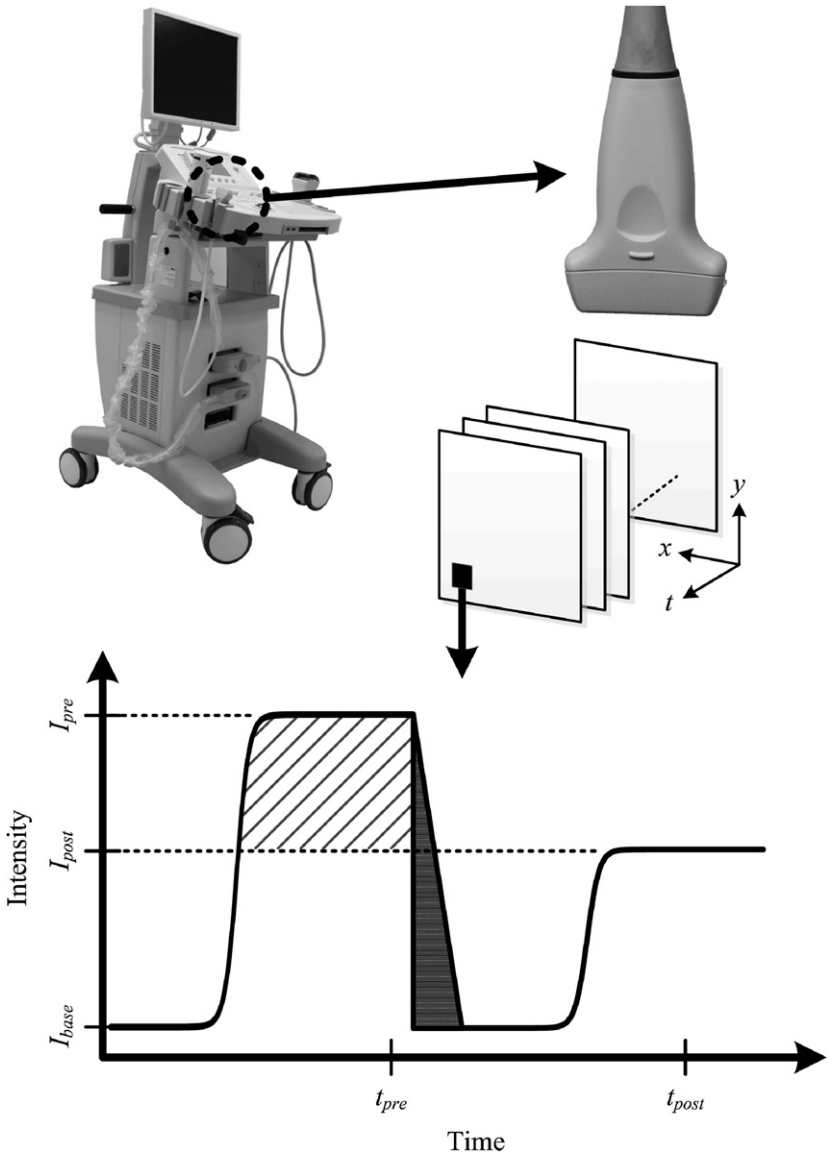

Fig. 2. Schematic of the low-intensity ultrasound imaging and processing strategy used to determine targeted microbubble (MB) binding to Ad-HA-GFP induced receptors. As MBs flow into the tumor, image intensity attributable to MB influx and binding increases (I_{pre}). A high-intensity flash image sequence destroys both circulating and bound MBs from a region-of-interest. Subsequently, systemically flowing MBs replenish the tumor vasculature (I_{post}) within a few seconds. The average image intensity attributed to targeted MB accumulation (dashed region) can be calculated by digital subtraction of registered image frames at pre-flash (t_{pre}) and post-flash (t_{post}) time points. Ad-HA-GFP = adenoviral-hemagglutinin-green fluorescent protein.

on control tumors or 24 h after low or high Ad dosing ($N = 4$ per group). Specifically, fluorescence imaging of excised tumor samples and target receptor density levels was completed using a 1-s exposure, binning of 4, and F/stop of 1. These parameters were chosen to optimize GFP signal visualization and to prevent image over-saturation. A fixed-size ROI was used to circumscribe each tumor depicted in the fluorescent images and normalized GFP expression was recorded as photons/s.

Remaining excised tumors ($N = 6$) underwent immunohistologic processing to verify target receptor protein expression and spatial variability. Tumor samples were placed in 10% phosphate buffered formalin for a 24-h period. Tumors were then embedded in paraffin tissue blocks, sliced, and dried overnight at 60°C. A hematoxylin and eosin (H&E) stained section was obtained from each tissue block. All sections subject to immunohistochemistry were deparaffinized and hydrated with deionized water. The tissue sections were heat

treated with 0.01M Tris-1mM EDTA buffer (pH 9.0) using a pressure cooker (CEPC 800; Cook's Essentials, China) for 5 min at maximum pressure (15 lb/in^2). Following antigen retrieval, all sections were gently washed in deionized water and then transferred to TBST (0.05M Tris-based solution in 0.15M NaCl with 0.1% v/v Triton-X-100, pH 7.6). Endogenous peroxidase was blocked with 3% hydrogen peroxide for 10 min. To further reduce non-specific background staining, slides were incubated with 3% normal goat or horse serum for 20 min (Sigma, St. Louis, MO, USA). All slides were then incubated at 4°C overnight with anti-HA antibody. Negative controls were achieved by eliminating the primary antibodies from the diluents. Diaminobenzidine (DAB, Scy Tek Laboratories, Logan, UT, USA) was used as the chromagen and hematoxylin (7211; Richard-Allen Scientific, Kalamazoo, MI, USA) as the counterstain.

Statistical analysis

All experimental data was summarized as mean ± SE and reported as percent change. A two-sample paired *t*-test was used to calculate statistical differences between control and targeted MB groups and low and high Ad-HA-GFP vector dosed groups. A p value of less than 0.05 was considered statistically significant. Data was analyzed using Excel (Microsoft Corp, Redmond, WA, USA).

RESULTS

Experiments were conducted to determine if serial changes in intratumoral Ad-HA-GFP vector dosing modulates intratumoral receptor expression as assessed using molecular US imaging. Intratumoral ROI analysis of contrast-enhanced US images provides a basis of determining receptor expression and MB binding to the intravascular target. Representative contrast-enhanced US imaging results using targeted and control MBs after both low and high Ad-HA-GFP vector dosing are illustrated in Figure 3. As shown, US imaging of targeted MBs improves contrast levels compared with control MB imaging. Note that pre-flash images after high Ad-HA-GFP vector dosing (day 2) show greater intratumoral enhancement than that found after low Ad-HA-GFP vector dosing (day 1). Post-flash images exhibit no discernible differences indicating that all bound MBs were removed from the imaging plane leaving only systemically circulating agents.

Compared with control, targeted MB imaging on day 1 (following low Ad-HA-GFP vector dose) showed a 1053.0% increase in intratumoral image intensity. On day 2 (after high Ad-HA-GFP dosing), molecular US imaging with the same anti-HA antibody-labeled MBs exhibited an 1880.4% increase in image intensity over control MB imaging results. Intratumoral enhancement attributable to targeted MB binding and accumulation was significantly increased over non-targeted (control) MB contrast enhancement on both days ($p < 0.001$). ROI analysis of targeted MB-based images from day 1 and 2 showed a mean intensity of $1.2 \times 10^6 \pm 2.1 \times 10^5$ and $1.7 \times 10^6 \pm 2.5 \times 10^5$, respectively. As detailed in Figure 4, intratumoral targeted MB binding after high Ad-HA-GFP vector dosing (day 2) was significantly higher than that found after low Ad vector dosing (day 1) ($p = 0.001$) confirming that a higher Ad-HA-GFP vector dose increased receptor expression and targeted MB accumulation. The average change in HA-targeted MB accumulation from day 1 to day 2 was 57.4%. Increases in targeted MB binding from each of the six animals studied are illustrated in Figure 5. With exception to animal one, intratumoral enhancement from day 1 to day 2 was relatively consistent between animals demonstrating reproducibility of the Ad-HA-GFP vector dosing technique for target receptor promotion.

Mean ROI intensities derived from control MB images were $1.0 \times 10^5 \pm 6.2 \times 10^4$ and $8.7 \times 10^4 \pm 5.0 \times 10^4$ for day 1 and day 2, respectively. Note that intensity values from control MB images were at least one order of magnitude lower than that found from US imaging the same animal population with targeted MBs. Comparison of US imaging results using control MBs revealed no significant differences between day 1 and day 2 ($p = 0.96$), showing consistency in MB injections and non-specific binding characteristics.

Quantification of the induced target receptors was possible with fluorescence imaging because of the intrinsic GFP expression produced by the Ad-HA-GFP vector. Figure 6 summarizes intratumoral target receptor levels in control animals (no Ad dose) and in low and high Ad dosed tumors. Control tumors were imaged to determine the presence of any background GFP signal, or autofluorescence, in the excised tissue. Low Ad dosed tumors had an average fluorescence of $3.53 \times 10^9 \pm 3.11 \times 10^8$ photons/s. Meanwhile, high Ad dosed tumors exhibited an average fluorescence of $6.80 \times 10^9 \pm 3.09 \times 10^9$ photons/s, or a 48% increase in target receptor expression compared to low Ad dosed tumors ($p = 0.33$). A small sample size prevented a significant difference between low and high expression, however, tumors injected with the control dosage (no Ad-HA-GFP virus) exhibited an average fluorescence of $1.97 \times 10^9 \pm 1.79 \times 10^8$ photons/s, which was significantly less compared with both the high ($p = 0.04$) and low ($p = 0.001$) Ad dosed tumors and target receptor levels.

Figure 7 displays representative H&E and HA immunohistologic sectional stains. Inspection of H&E

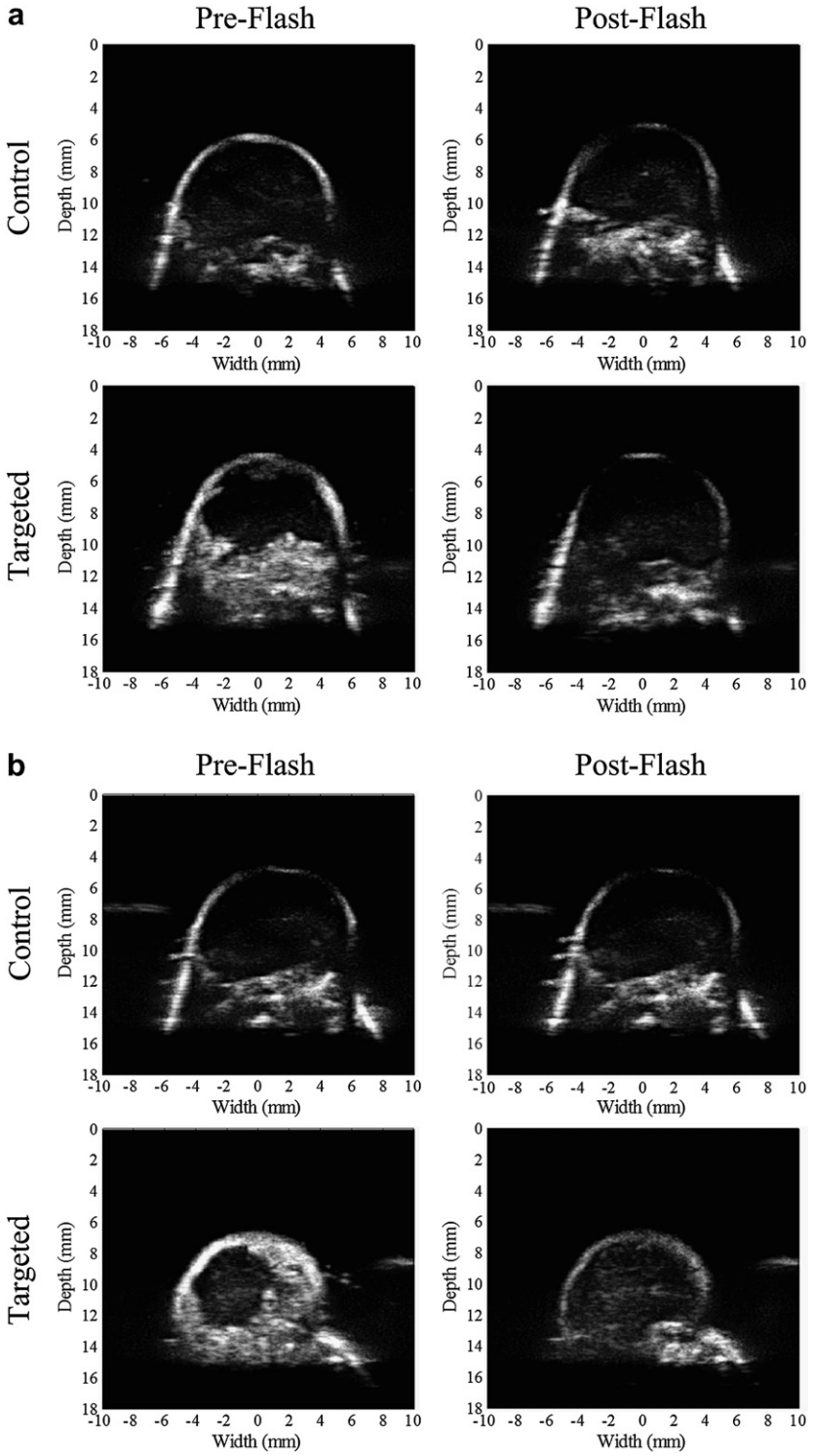

Fig. 3. (a) Representative ultrasound images acquired using control and hemagglutinin (HA)-targeted microbubbles (MBs) after low dose Ad-HA-GFP vector infection (day 1). (b) Susequently, animals were administered a high dose Ad-HA-GFP vector intratumoral injection and ultrasound imaging with control and HA-targeted MBs was repeated (day 2). Ad-HA-GFP = adenoviral-hemagglutinin-green fluorescent protein.

sections reveals a characteristic pattern of central necrosis in a majority of the tumor cross sections. Notwithstanding, H&E sections consistently depict viable tissue in the peripheral portion of the tumors and those regions stained positive for the target HA protein. These immunohistologic results confirm successful

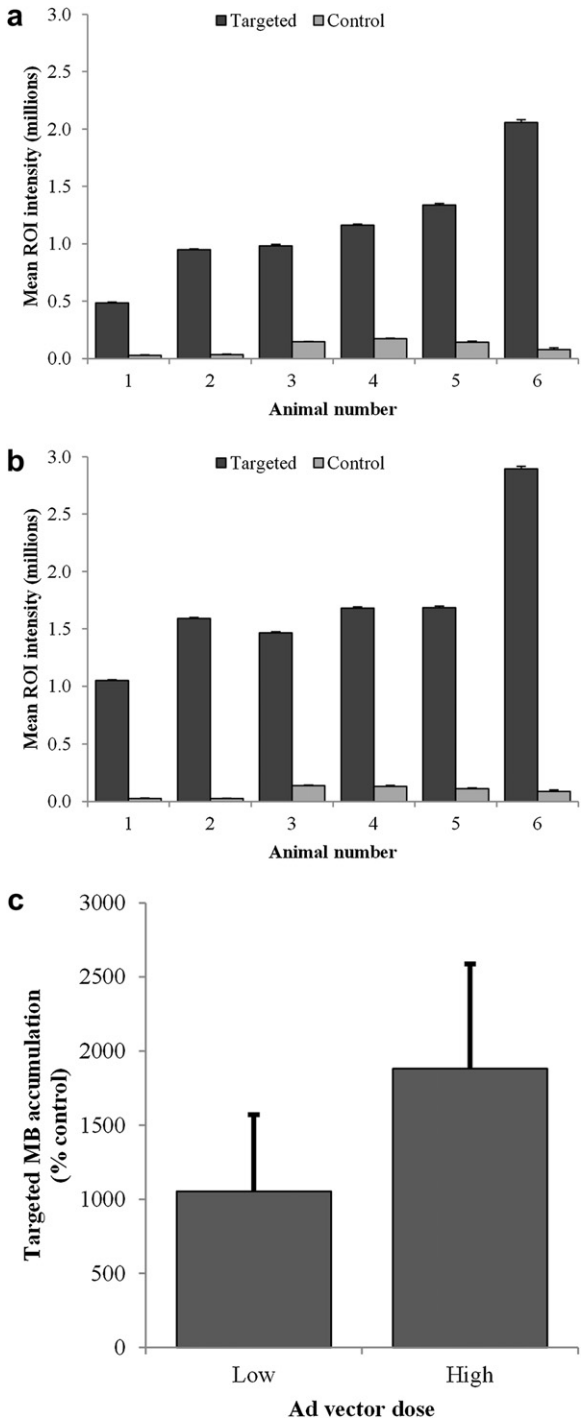

Fig. 4. Intratumoral targeted and control microbubble (MB) accumulation after (a) Low dose and (b) High dose Ad-HA-GFP vector infection. MB accumulation was calculated through digital subtraction of pre-flash and post-flash frames then averaging ROI pixel intensity values. Increasing the Ad vector dose increased receptor expression and MB accumulation. (c) Targeted MB data was averaged for all animals and normalized to control values to show the percent increase between low (day 1) and high (day 2) Ad-HA-GFP dosing. Ad-HA-GFP = adenoviral-hemagglutinin-green fluorescent protein.

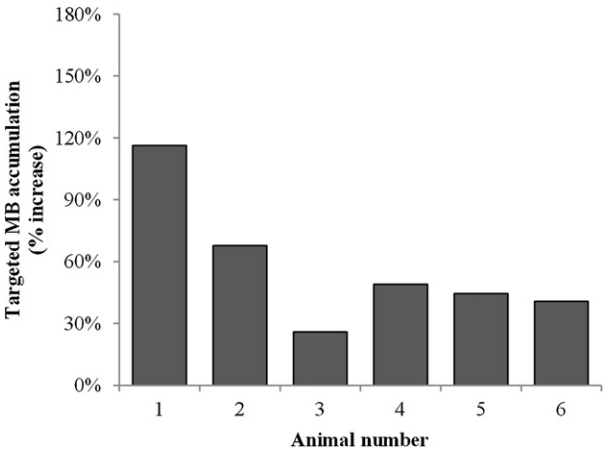

Fig. 5. Percent increases in intratumoral targeted microbubble (MB) accumulation for each animal after low (day 1) to and high (day 2) Ad-HA-GFP vector dosing. Data was obtained by averaging intratumoral image intensity values for each day and calculating the percent change. Ad-HA-GFP = adenoviral-hemagglutinin-green fluorescent protein.

Ad-HA-GFP vector infection and homogeneous intratumoral HA expression in viable tissue.

DISCUSSION

In this study, we evaluated the *in vivo* efficacy of a model system using Ad vector modulation of an intratumoral HA protein. Traditionally, targeted MB studies have used different cell lines to verify MB binding to

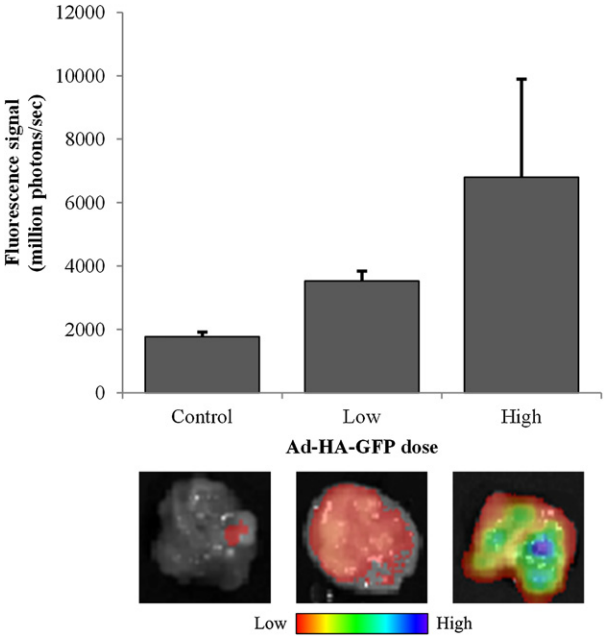

Fig. 6. Fluorescence imaging of tumors injected with a high, low, or no Ad-HA-GFP vector. GFP signal was collected as photons/sec from the three different groups. Ad-HA-GFP = adenoviral-hemagglutinin-green fluorescent protein.

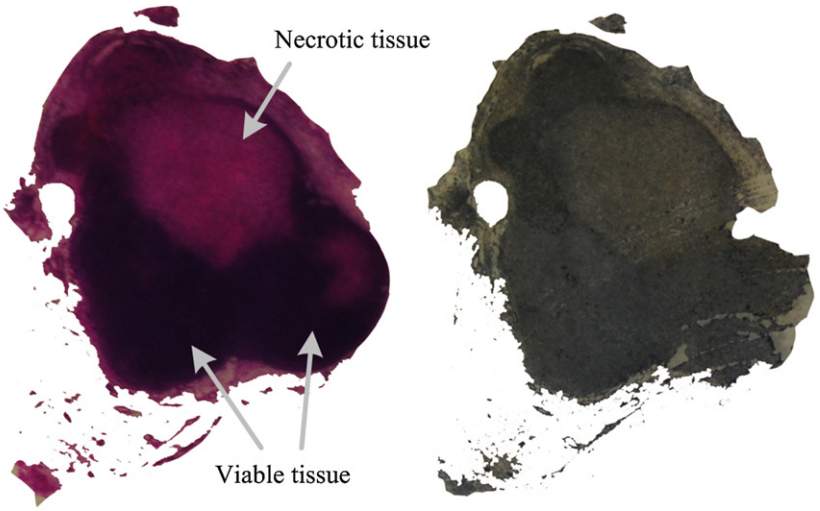

Fig. 7. Representative histologic sections from excised tumor samples. An H&E stain was performed to analyze viable intratumoral regions and necrotic areas (left). A stain for the hemagglutinin (HA) receptor was performed and homogeneous target receptor expression can be seen on the peripheral (darker) region of the tumor (right). The necrotic core of the tumor has little or no HA receptor expression.

overexpressed receptors found in tissue states of disease. While convenient, the use of different cell lines in animal implantation and experimentation introduces considerable variation in tumor yield, cell line proliferation rates and tumor growth and metastatic ability. The use of Ad vectors to control and modulate receptor expression offers the ability to conduct molecular US imaging studies using the same cell line so the above noted variations are minimized. Without any bias of varying receptor expression, the mechanisms behind molecular US imaging are more easily explored using this model system.

Previously, we investigated the use of Ad vectors for modulating receptor expression and targeted MB binding in an *in vitro* study (Saini et al. 2011). Results showed a linear response between increased Ad-HA-GFP vector dose and receptor expression in the 2LMP breast cancer cell line. Additionally, it was shown that HA-targeted MB attachment was proportional to receptor density. This study concluded that the Ad vector approach is an ideal model to verify and analyze *in vitro* targeted MB performance.

For *in vivo* evaluation, viral infection occurred intratumorally and targeted MB "flash" sequences were used for the US imaging technique. This sequence has been widely used to quantify targeted MB binding *in vivo* because it allows for direct measurement of MB accumulation in the vessels. Adherent MBs are quantitatively assessed by subtracting post-flash intensities from the pre-flash intensities (Willmann et al. 2008). By modulating the Ad-HA-hSSTr2-GFP vector dose, expression of the exogenous cellular receptor (HA protein) within the tumor at low and high concentrations was achieved (Zinn et al. 2002). *In vivo* results showed that the HA-targeted MB frame intensity difference was significantly different for day 2 (high Ad-HA-GFP vector dose) than for day 1 (low Ad-HA-GFP dose). For IgG isotype control MBs, signal enhancement attributable to MB accumulation relative to HA-targeted MB was considerably lower. Therefore, MB accumulation is proportional viral dose and expression levels of the induced receptors *in vivo*. Additionally, fluorescence imaging confirmed that high Ad vector dosing increases GFP expression, hence, more target proteins induced, compared with the low and no Ad vector dosing. The spatial distribution of the MB contrast enhancement was seen mostly in the tumor periphery. Weller et al. and Korpanty et al. have similarly shown peripheral enhancement to correlate with viable tissue (Korpanty et al. 2007; Weller et al. 2005). Future work would incorporate histologic analysis to correlate hyperechoic regions with viable tissues for further quantitative analysis of targeted MBs.

Due to the nature of the fixed circular ROI for image analysis, extratumoral intensities could have been included in the analysis, therefore, skewing results. One limitation to this study was that due to slight variation in positioning of the US probe, tumor cross-sections of the animals were not known to be consistent from day 1 to day 2. Therefore, the radius of the circular ROI was slightly different from day 1 to day 2. However, ROI radius and time points after MB injections were held constant between each mouse for both targeted and control MB imaging sessions. Additionally, the order of the ad-injection (low dose followed by a high dose after the imaging session) might have brought bias during

experimentation, however, the order of the Ad vector dose allowed for a longitudinal study of the induced receptors while having a consistent tumor size and population for targeted and control MB imaging between the 2 days. Also, the lack of control mice without adenoviral dose was not present for quantitative analysis.

If receptor density increases (or decreases) during disease progression, molecular US imaging of targeted MBs can be useful for characterizing the diseased tissue. The model system introduced can be used extensively in preclinical molecular US imaging studies where minimal biologic variation in tumor-bearing animals is desirable. The correlation established between MB accumulation and increased cellular receptors may be useful in applications like receptor profiling and/or therapeutic monitoring. Presently, clinical translation of targeted MBs with the streptavidin-biotin bridge to conjugate MBs and antibody is not possible because of a strong immunogenic response in human. However, some groups have recently fabricated a MB with an alternate binding chemistry to avoid immunogenic response and, thus, have potential for clinical application (Pysz et al. 2010b; Willmann et al. 2010; Bzyl et al. 2011; Pochon et al. 2011).

In conclusion, the results of this study verified a model system using Ad vector techniques to modulate receptor protein expression and quantify targeted MB accumulation *in vivo* using molecular US imaging.

REFERENCES

Bachmann C, Klibanov AL, Olson TS, Sonnenschein JR, Rivera-Nieves J, Cominelli F, Ley KF, Lindner JR, Pizarro TT. Targeting mucosal addressing cellular adhesion molecular (MAdCAM)-1 to noninvasively image experimental Crohn's disease. Gasteroenterology 2006;130:8–16.

Bzyl J, Lederle W, Rix A, Grouls C, Tardy I, Pochon S, Siepmann M, Penzkofer T, Schneider M, Kiessling F, Palmowski M. Molecular and functional ultrasound imaging in differently aggressive breast cancer xenografts using two novel ultrasound contrast agents (BR55 and BR38). Eur Radiol 2011;21:1988–1995.

Ferrante EA, Pickard JE, Rychak J, Klibanov A, Ley K. Dual targeting improves microbubble contrast agent adhesion to VCAM-1 and P-selectin under flow. J Control Release 2009;140:100–107.

Kaufmann BA. Ultrasound molecular imaging of atherosclerosis. Cardiovasc Res 2009;83:617–625.

Kaufmann BA, Carr CL, Belcick JT, Xie A, Yue Q, Chadderdon S, Caplan ES, Khangura J, Bullens S, Bunting S, Lindner JR. Molecular imaging of the initial inflammatory response in atherosclerosis: Implications for early detection of disease. Ateriosclr Thromb Vasc Bio 2009;30:54–59.

Klibanov AL. Ligand-carrying gas-filled microbubbles: Ultrasound contrast agents for targeted molecular imaging. Bioconjugate Chem 2005;16:9–17.

Korpanty G, Carbon JG, Grayburn PA, Fleming JB, Brekken RA. Monitoring response to anticancer therapy by targeting microbubbles to tumor vasculature. Clin Cancer Res 2007;13:323.

Knowles JA, Heath CH, Saini R, Umphrey H, Warram J, Hoyt K, Rosenthal E. Molecular targeting of ultrasound contrast agent for detection of head and neck squamous cell carcinoma. Arch Otolaryngol Head Neck Surg 2012;138:662–668.

Leighton TG. The acoustic bubble. London: Academic Press; 1997.

Pochon S, Tardy I, Bussat P, Bettinger T, Brochot J, von Wrongski M, Passantino L, Schneider M. BR55: A lipopetide-based VEGFR2-targeted ultrasound contrast agent for molecular imaging of angiogenesis. Invest Radiol 2011;45:89–95.

Pysz MA, Foygel K, Rosenberg J, Gambhir SS, Schneider M, Willmann JK. Antiangiogenic cancer therapy: Monitoring with molecular US and a clinically translatable contrast agent (BR55). Radiology 2010a;256:519–527.

Pysz MA, Gambhir SS, Willmann JK. Molecular imaging: Current status and emerging strategies. Clin Radiol 2010b;65:500–516.

Pysz MA, Willmann JK. Targeted contrast-enhanced ultrasound: an emerging technology in abdominal and pelvic imaging. Gasteroenterology 2011;140:785–790.

Rogers BE, Chaudhuri TR, Reynolds PN, Della Manna D, Zinn KR. Noninvasive gamma camera imaging of gene transfer using an adenoviral vector encoding an epitope-tagged receptor as a reporter. Gene Ther 2003;10:105–114.

Saini R, Sorace AG, Warram J, Umphrey H, Zinn K, Hoyt K. Model system using controlled receptor expression for evaluating targeted ultrasound contrast agents. Ultrasound Med Biol 2011;37:1306–1313.

Schumann PA, Chirstiansen JP, Quigley RM, McCreery TP, Sweitzer RH, Unger EC, Linder JR, Matsunaga TO. Targeted-microbubble binding selectively to GPIIb IIIa receptors of platelet thrombi. Invest Radiol 2002;37:587–593.

Wang B, Zang WJ, Wang M, Ai H, Wang YW, Li YP, He GS, Yu XJ. Prolonging the ultrasound signal enhancement from thrombi using targeted microbubbles based on sulfur-hexafluoride-filled gas. Acad Radiol 2006;13:428–433.

Warram JM, Sorace AG, Saini R, Umphrey H, Zinn KR, Hoyt K. Triple-targeted US contrast agent provides improved localization to tumor vasculature. J Ultrasound Med 2011;30:921–931.

Warram JM, Sorace AG, Saini R, Borovjagin AV, Hoyt K, Zinn KR. Systemic delivery of a breast cancer-detecting adenovirus using targeted microbubbles. Cancer Gene Ther 2012;19:545–552.

Weller GE, Wong MK, Modzelewski RA, Lu E, Klibanov AL, Wagner WR, Villanueva FS. Ultrasonic imaging of tumor angiogenesis using contrast microbubbles targeted via the tumor-binding peptide arginine-arginine-leucine. Cancer Res 2005;65:533–539.

Willmann JK, Paulmurugan R, Chen K, Gheysens O, Rodriguez-Porcel M, Lutz AM, Chen IY, Chen X, Gambhir SS. US imaging of tumor angiogenesis with microbubbles targeted to vascular endothelial growth factor receptor type 2 in mice. Radiology 2008;246:508–518.

Willmann JK, Kimura RH, Deshpande N, Lutz AM, Cochran JR, Gambhir SS. Targeted contrast-enhanced ultrasound imaging of tumor angiogenesis with contrast microbubbles conjugated to integrin-binding knottin peptides. J Nucl Med 2010;51:433–440.

Zinn KR, Chaudhuri TR, Krasnykh VN, Buchsbaum DJ, Belousova N, Grizzle WE, Curlel DT, Rogers BE. Gamma camera dual imaging with a somatostatin receptor and thymidine kinase after gene transfer with a bicistronic adenovirus in mice. Radiology 2002;223:417–425.